INWARD RECTIFICATION The final class of K^+ currents (which includes mixed cation currents), are tonically active at subthreshold membrane potentials, are activated by *hyperpolarization* rather than depolarization, and do not inactivate. The slow mixed-cation (Na^+/K^+) current I_H (also sometimes known as I_Q) underlies slow oscillatory behavior in several cell types and has been shown to be present in neocortical pyramidal neurons and to contribute to subthreshold membrane resonance (Spain, Schwindt, and Crill 1990; Perkins and Wong 1995; Hutcheon, Miura, and Puil 1996a, 1996b). The anomalous rectifying K^+ current, I_{IR} has similar properties to I_H, but with much faster kinetics (Constanti and Galvan 1983; Sutor and Hablitz 1993).

The inwardly rectifying currents belong to a relatively large class of K^+ channels, known logically as the "inward rectifier family" (Kir; reviewed in Doupnik, Davidson, and Lester 1995). Not much is known about the subcellular distribution of these channels. Based on dendritic recordings and modeling of subthreshold oscillations in neocortical pyramidal neurons, Hutcheon, Miura, and Puil (1996a) argued for the presence of I_H in the dendrites (as well as the soma). Because the inward rectifiers are tonically active at resting membrane potentials, a nonuniform distribution of these channels would result in an effectively nonuniform membrane resistance. The possibility of dendritic membrane enriched in I_H or I_{IR} could complicate substantially the interpretation of passive membrane models. Based on a study combining dual somatic/dendritic recordings and compartmental modeling, Spruston and Stuart (1996) have suggested that I_H may indeed be concentrated in the apical dendrite.

5.2.6 Axonal Structure and Function

In a passive compartmental model, the axon contributes very little to dendritic or somatic behavior because its fine caliber and electrical isolation from the remainder of the cell produce little passive load (Rall et al. 1992). In models with active properties, however, the axon (or at least its proximal segments) may contribute substantially to the behavior of the neuron due to the contribution of voltage-gated Na^+ channels that make the axon the site of action potential initiation (Coombs, Curtis, and Eccles 1957a; Stuart and Sakmann 1994; Spruston, 1995; Colbert and Johnston 1996). Although the majority of published compartmental models omit the axon, several recent models of pyramidal cells have incorporated axonal anatomy as an essential component (e.g., Traub et al. 1994; Mainen et al. 1995; Rapp, Yarom, and Segev 1996).

Anatomy In pyramidal cells, the axon arises from the soma or in some cases from a basal dendrite. The transitional region where the axon meets the soma is known as

the "axon hillock." The *initial segment* of the axon is an ultrastructurally specialized region that generally extends to the first myelinated segment and is the target of about 20–50 axoaxonic inhibitory synapses (Peters, Proskauer, and Kaiserman-Abramof 1968; Jones and Powell 1969; Fariñas and DeFelipe 1991) made by a special class of GABA-ergic inhibitory interneurons called "chandelier cells" (Somogyi, Freund, and Cowey 1982).

In pyramidal neurons of the neocortex and hippocampus, the length of the initial segment ranges from about 20 μm to 50 μm (Sloper and Powell 1978; Somogyi, Freund, and Cowey 1982; Fariñas and DeFelipe 1991; Colbert and Johnston 1996) with an average diameter in the range of 1–2.5 μm (Westrum 1970; Fariñas and DeFelipe 1991). There is generally a 2- to 4-fold taper from the hillock to the distal end (Fariñas and DeFelipe 1991).

In myelinated axons, the myelin sheath begins at the end of the initial segment and is interrupted regularly by the nodes of Ranvier. In the terminal arbors of cat cortical axons, an internodal length of around 100 μm is typical (Waxman and Melker 1971; Deschênes and Landry 1980a), but systematic studies of internodal lengths of proximal axonal arbors are not available. The myelinated segments are thicker than the initial segment or nodes of Ranvier (Palay et al. 1968), with diameters in the range of 0.5–2 μm (Haug 1968). It is also important to note that myelination is only partially developed in the juvenile rats used in many electrophysiological studies.

Sodium Channels The propagation of nerve impulses in myelinated axons depends critically on localization of Na^+ channels to the nodes of Ranvier (Black, Kocsis, and Waxman 1990). Similarly, localization of Na^+ channels to the axon initial segment (Angelides et al. 1988; Kobayashi et al. 1992) has been proposed to contribute to the role of this structure as the site of action potential initiation (Coombs, Curtis, and Eccles 1957a; Dodge and Cooley 1973; Mainen et al. 1995; Rapp, Yarom, and Segev 1996). A primary distinguishing feature of both the initial segment and the nodes of Ranvier is the presence of an electron-dense undercoating (Peters, Proskaucr, and Kaiserman-Abramof 1968), which has long been thought to be related to electrical conduction (Peters, Proskauer, and Kaisermann-Abramof 1968; Palay et al. 1968), presumably reflecting to an elevated density of Na^+ channels. The existence of structural barriers to diffusion of Na^+ channels between the axon hillock and soma (Srinivasan et al. 1988; Kobayashi et al. 1992) could provide the molecular basis for the trapping of channels in the initial segment. Conventional estimates of nodal Na^+ channel density are 1,000–2,000 channels/μm^2, compared with a 30-fold lower density in internodal regions (Black, Kocsis, and Waxman

1990; Waxman and Ritchie 1993). But is there a similar difference in channel density between soma and initial segment?

Measurements with fluorescent toxin–binding studies (Angelides et al. 1988) have shown up to 30-fold higher Na^+ channel density in the initial segment compared to the soma in cultured spinal cord neurons, consistent with the analogy to node and internode, although lower differences (<10-fold) were found in cortical neurons (Angelides et al. 1988) and retinal ganglion cells (Wollner and Catterall 1986). Moreover, using direct patch clamp recordings from the initial segments of subicular pyramidal cells, Colbert and Johnston (1996) found *no difference* between somatic and initial segment densities. Because the Na^+ channels of the initial segment may be clustered (Angelides et al. 1988; Turner et al. 1994), it is possible that sampling problems hampered the patch clamp estimates. On the other hand, Colbert and Johnston (1996) also found no evidence for a substantially lower threshold at the initial segment compared to the soma, throwing considerable doubt on the applicability of the classical model to action potential initiation in pyramidal cells (see also below).

Other Properties Because of their small diameters, central axons are very difficult to measure electrophysiologically. There is consequently very little such data on axonal specializations of voltage-dependent channels or other electrical properties. As for dendrites, all major channel types are likely to be found in axonal membranes, albeit perhaps different subtypes at different densities. The presence of a variety of Ca^{2+} channels in axon terminals responsible for neurotransmitter release is well documented (reviewed in Reuter 1996). Various members of the Kv family of K^+ channels (corresponding to I_A and I_{Kd}) have been localized to axons in immunocytochemical studies.

Myelinated axon segments generally have very low capacitance (Black, Kocsis, and Waxman 1990; Hille 1992), for example, $0.04\,\mu F/cm^2$ (Graham and Redman 1994). While there may be very little leak current or other channels associated with myelinated axonal segments, the resistance of the nodes is believed in some cases to be substantially lower than even that of somatodendritic membrane (Blight 1985; Black, Kocsis, and Waxman 1990), for example, $50\,\Omega\,cm^2$ (Graham and Redman 1994). This lower resistance could help to repolarize the membrane following an action potential in the absence of a delayed rectifier current, although various K^+ channels are known to be present in axons (Sheng et al. 1992, 1994; Wang et al. 1994; Maletic-Savatic, Lenn, and Trimmer 1995; Weiser et al. 1995). In addition, several recent modeling studies have used lower axonal than dendritic axial resistivity, for example, 70–100 Ω cm versus 200–300 Ω cm (Traub et al. 1994; Rapp, Yarom, and

Segev 1996; Migliore 1996), although there is little experimental evidence to support a disparity.

Propagation Compared to dendritic processing, the subject of computation in the axons of pyramidal neurons has received relatively little attention (see reviews in Waxman 1975; Wall 1995). Three main classes of computation have been examined: (1) history-dependent spatiotemporal filtering of impulses (Chung, Raymond, and Lettvin 1970; Deschênes and Landry 1980b; Lüscher and Shiner 1990); (2) temporal delay processing (Manor, Koch, and Segev 1991); and (3) presynaptic inhibition of impulse conduction (Segev 1990; Graham and Redman 1994). These studies have been based on relatively simple models of action potential propagation (i.e., based on classical Hodgkin-Huxley Na^+ and K^+ currents), although evidence suggests that most of the channels contributing to the complexity of dendritic behavior are also present in axons. The potential impact of non-Hodgkin-Huxley channels on action potential conduction in axonal arbors (Lüscher et al. 1994b, 1994a) certainly bears further examination in compartmental models.

5.2.7 Exploring Parameters

From the data reviewed above, it is apparent that the practice of treating dendritic channel densities as free, unconstrained parameters is rapidly becoming untenable. It is nevertheless true that any model of a spatially extended neuron with active conductances will retain some degree of flexibility in assigning channel densities. Heterogeneity among cell subtypes and over developmental ages as well as variability across individual cells means that the idea of a canonical channel distribution will at best be a rough sketch. "Tuning" channel densities to fit a set of electrophysiological data will therefore be necessary. Indeed, this is considered to be the most arduous task in constructing a compartmental model and raises an interesting theoretical issue as to how each neuron determines and regulates these densities. One intriguing possibility is that local information in the time-varying membrane potentials and ion concentrations may control the local densities of particular channel types through up- and down-regulation as well as other biophysical mechanisms (Bell 1992; Siegel, Marder, and Abbot 1994 and chapter 10, this volume). The immediate concern of most modelers, however, is to find some way to constrain the parameters by matching simulations to experimental recordings.

In most studies, channel densities (and other parameters) are tuned by hand; that is, by trial and error, starting with plausible values for the parameters and changing them in some systematic way (e.g., Lytton and Sejnowski 1991; Traub et al. 1991, 1994; Rhodes and Gray 1994; Migliore, Alicata, and Ayala 1995; Mainen and

Sejnowski 1996). Although, in some cases, individual parameters may be directly related to specific electrophysiological variables, the correspondence is seldom simple: most behaviors are the net result of the interaction of multiple currents with the electrotonic structure of the neuron (Mainen and Sejnowski 1996). There is very little explicit description in the modeling literature about how the process of parameter tuning is carried out. In the best cases, a particular final set of channel densities is loosely justified in terms of direct measurements and their effects on net electrophysiolgical behavior (e.g., Traub and Llinás 1979, Traub 1982; Traub et al. 1985, 1991; Quadroni and Knöpfel 1994). A promising approach in this regard is the use of a combination of in vitro and in vivo recordings from the same cell type: constraints can be added progressively, starting with in vitro recordings from dissociated neurons without dendrites, and proceeding to recordings from a slice preparation in which the dendrites are present but there is minimal synaptic activity, and finally to in vivo recordings from neurons that reflect the full complexity of a dynamic, nonstationary environment (Destexhe et al. 1996).

A number of attempts to systematize the process of parameter tuning have been described (e.g., Foster, Ungar, and Schwaber 1993; Bhalla and Bower 1993; Eichler-West and Wilcox 1995; Baldi, Vanier, and Bower 1996). The number of combinations of parameters that must be searched goes up exponentially with the number of parameters, so that in even the simplest one-compartment model with a few dozen parameters, an exhaustive search over all possible combination is simply not feasible. While there are ways to find optimal combinations of parameters in high-dimensional spaces, they suffer from both local minimum and uniqueness problems. A set of parameters may be locally optimal in the sense that making small changes to the parameters increases the error of the fit (Bhalla and Bower 1993), but there may be a better overall set of parameters in a different part of the parameter space that has not been tested. An approach based on genetic algorithms offers a way to make large jumps in the values of some combinations of parameters (Eichler-West and Wilcox 1995). The problem with uniqueness is that there may be many combinations of parameter values that fit the limited data equally well. Without a sufficiently rich set of data to constrain all the parameters in the model, it is impossible to have any confidence in the interpretation of the model.

The primary difficulty of systematic approaches based on optimization has been the time required to compute a single "evaluation function" (i.e., a simulation run) —typically seconds. Increases in computer performance are making these approaches more practical. In particular, the fastest supercomputers are multiple instruction, multiple data (MIMD) machines that have thousands of microprocessors. Because each processor can run the same simulation program with a different set of parame-

ters, taking full advantage of the computational power in a data-parallel way, these machines are ideal for exploring parameter spaces (see chapter 12, this volume).

A few general points are worth mentioning about confronting a complex model with thousands of parameters. First, there is a wide choice for the evaluation function, ranging from timing the occurrences of action potentials in response to current injection to matching statistical measures such as current-frequency curves (Foster, Ungar, and Schwaber 1993). Second, experimental data from a variety of conditions are needed to constrain most models, e.g., including the responses of neocortical neurons to fluctuating current injection, which is closer to in vivo conditions, as well as more conventional step current pulses (Mainen and Sejnowski 1995; Tang, Bartels, and Sejnowski 1997). Third, the problem of searching the space can be reduced to some extent by identifying parameters that covary; that is, the result may depend only on the ratios of some parameters, or on some other functional combination. A Bayesian framework offers a systematic way to take such dependencies into account (Baldi, Vanier, and Bower 1996). The most highly sensitive parameters in reproducing a particular result may be the most critical ones to constrain experimentally, and this may be one of the most important insights gained from the model.

Finally, if the goal of a model is to make a new discovery, in addition to summarizing existing data, the search for anomalies and failures of the model to fit aspects of the data may be more important than finding a perfect fit. When a model fails, the assumptions that went into constructing the model must be critically assessed, which can lead to new insights.

5.3 Applications

This section presents a few selected applications of compartmental models that have explored active dendritic function. Several examples have been chosen to illustrate how a detailed model helped to guide or illuminate electrophysiological studies along three lines of investigation: (1) synaptic integration in dendrites; (2) spike initiation and dendritic propagation; and (3) generation of firing patterns.

5.3.1 Synaptic Integration

Historically, dendrites have been seen as impeding current flow from synapses to the soma (Rinzel and Rall 1974). As a number of modeling studies have shown, synaptic inputs to distal dendritic locations suffer considerable attenuation in passive dendritic arbors of reconstructed neurons (Spruston et al. 1993; Zador, Agmon-Snir, and Segev 1995; Major et al. 1994; Mainen et al. 1996). A major role for excitable dendritic currents has been seen in boosting distal synaptic input to enhance its

propagation to the soma (Perkel and Perkel 1985; Shepherd et al. 1985; Pongracz 1985; Segev and Rall 1988; Jaslove 1992; Wathey et al. 1992).

The problem of synaptic attenuation and the possible role of active currents was addressed by Connors and colleagues (Cauller and Connors 1992; Amitai et al. 1993; Cauller and Connors 1994). Although it was found electrophysiologically that stimulation of layer-1 input to the distal tuft of layer-5 pyramidal cells could produce a surprisingly strong somatic excitatory postsynaptic potential (EPSP), a model neuron with a passive dendritic tree and massive layer-1 input could not reproduce a somatic EPSP as large as those observed experimentally (figure 5.2). Two problems contributed to weakening the effects of distal input on the soma:

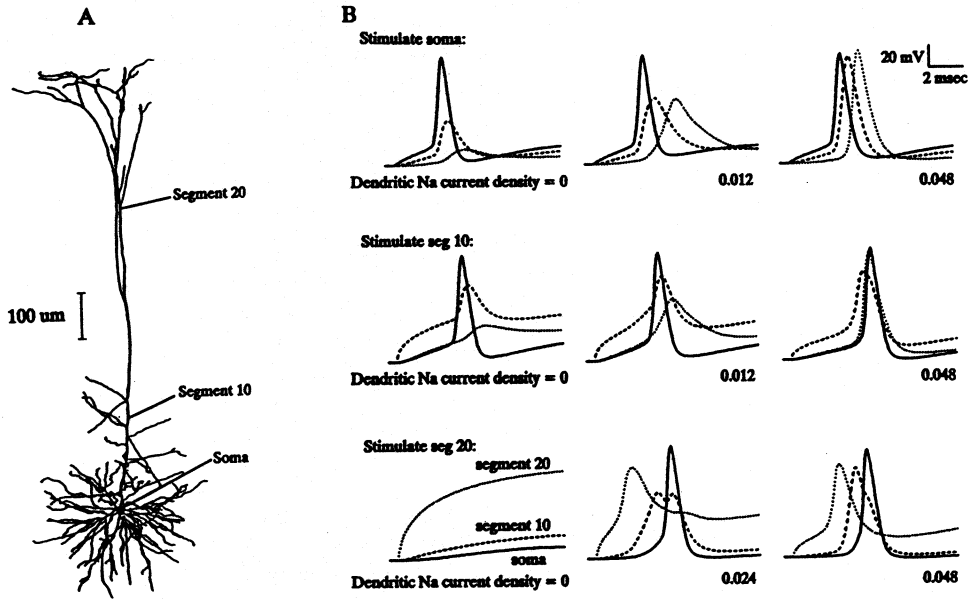

Figure 5.2
Simulations of soma-dendritic Na^+ spiking in a layer-5 pyramidal cell. (A) Camera lucida drawing of the modeled cell. Labels designate the locations of the three sites from which voltage charges are illustrated in panel B. (B) Effects of dendritic Na^+ channels and stimulus site on dendritic spiking; superimposed voltage responses from the soma (solid line), the trunk of the apical dendrite (segment 10; dashed line), and the end of apical trunk (segment 20; dotted line) while simulating with a step depolarizing pulse of current (intensity adjusted in each case to 1.5 times somatic spike threshold). Current was applied either at the soma (top row), to segment 10 (middle row), or to segment 20 (bottom row). Active Na^+ currents in the apical dendrites were assumed to be either absent (left column), at a relatively low density (middle column), or at a higher density (right column). Note that when the apical dendrites were passive (bottom left), it was not possible to bring the soma to spike threshold by stimulating segment 20, even when the local dendritic potential was positive.

1. The relatively high impedance of the distal branches leads to saturation of the synaptic current as the local membrane potential quickly depolarizes the neuron to near the synaptic reversal potential.
2. The cable properties (particularly the large axial resistance) of the dendritic arbor produce a large voltage drop between the distal site and the soma.

This anomaly between the model and the experimental results led to the hypothesis that low densities of Na^+ channels in the apical dendrite could boost layer-1 input enough to fire the cell (Cauller and Connors 1992; Amitai et al. 1993; Cauller and Connors 1994). This circumvents problem 2 by a counteracting the voltage drop along the apical dendrite. Bernander, Koch, and Douglas (1994) expanded on this idea by tackling problem 1 in addition to problem 2. By adding a depolarization-activated outward current to the apical dendrite, their model compensated for saturation of synaptic current, helping to counteract the local depolarization produced by large inputs. They derived the voltage-dependence of a K^+ current necessary to accomplish exact linearization and showed that a biophysically reasonable K^+ current would be roughly suitable. Thus, in principle, a combination of Na^+ boosting and K^+ linearization could serve to compensate for the effects of the passive cable properties on synaptic input.

Recently, several physiological studies have directly tested the actual contribution of Na^+ currents to synaptic potentials (Stuart and Sakmann 1995; Schwindt and Crill 1995; Lipowsky, Gillessen, and Alzheimer 1996). Studying CA1 neurons, Lipowsky, Gillessen, and Alzheimer (1996) demonstrated that the amplitude of distal synaptic EPSPs, measured at the soma, was reduced by tetrodotoxin (TTX) locally applied to the apical dendrite (and to a much lesser extent by TTX applied to the axon or soma). Interestingly, the shape of the EPSP was not affected by TTX. To ensure that TTX was not acting presynaptically (TTX blocks presynaptic action potentials as well as postsynaptic Na^+ channels), they used a local field potential recording of the synaptic current (which was not affected by TTX) and postsynaptic hyperpolarization (which reduced the observed boosting). Examined in a compartmental model, these observations were consistent with physiological densities of I_{Na} in the main apical dendrite. Moreover, a dendritically located low-voltage-activated K^+ current was also needed to reproduce the data: specifically, to account for the lack of significant shape change of the boosted EPSPs.

In a study of layer-5 pyramidal cells, Stuart and Spruston (1995) also demonstrated the ability of a persistent Na^+ current to boost subthreshold synaptic currents, although they arrived at somewhat different conclusions about the location of the Na^+ channels contributing to the synaptic boost. Their technique was to use a

dendritic patch clamp electrode to inject current into the dendrite to mimic a synaptic current. This allowed them to use TTX to block I_{Na_p}. Interestingly, using local TTX application, they found that axosomatic Na^+ channels had a much greater effect than dendritic Na^+ channels in boosting the subthreshold current injection. Furthermore, dual axonic and somatic recordings showed that the site of greatest amplification was in fact the axon rather than the soma, consistent with suggestions that the axon initial segment contains a high density of Na^+ channels (Mainen et al. 1995; see also section 5.3.2). Schwindt and Crill (1995) also showed a contribution of I_{Na_p} to subthreshold amplification in layer-5 cells by examining the effect of TTX on iontophoretically applied pulses of glutamate.

One interpretation of the differences between these studies is a significantly different distribution of Na^+ channels between cortical layer-5 pyramidal cell and hippocampal CA1 pyramidal cells (Lipowsky, Gillessen, and Alzheimer 1996). The neocortical pyramidal cells may have a relatively higher axonal density of Na^+ channels.

Given the complexity and variety of the voltage-dependent Na^+, Ca^{2+}, and K^+ channels in dendrites, the possibility arises that nonlinear synaptic integration more complex than amplification could occur. Even in the passive case, synaptic conductance changes could themselves cause current shunting and nonlinear interactions between nearby synapses (Rall 1964; Wang and Zhang 1996). Relative timing of a few milliseconds between neighboring excitatory and inhibitory synapses could significantly affect the current that reaches the spike-initiating region. (For a detailed model of the effects of voltage-dependent dendritic currents on synaptic integration in cerebellar Purkinje cells, see chapter 6, this volume.)

Before the properties of active dendritic conductances were firmly established, the theoretical possibility of performing logical operations (AND, OR, XOR) between synaptic inputs was explored with simulations (Shepherd and Brayton 1987; Rall and Segev 1987; Zador, Claiborne, and Brown 1992; Fromherz and Gaede 1993). A strictly logical function would be difficult to arrange, however, and low-order polynomial functions offer a more likely mathematical approximation to synaptic integration (Mel 1993). Sums of polynomial functions computed in different dendritic branches could be used to approximate a wide range of nonlinear functions, including the properties of complex cells in visual cortex (Mel, Ruderman, and Niebur 1996), which could be learned through long-term potentiation at excitatory synapses through activation of NMDA receptors (Mel 1992). This literature is necessarily more speculative and, thus far, less tied to physiological data (see Mel 1994 for a review). As recordings from dendrites become better refined, it should be possible to arrive at much better approximations to the types of spatial and temporal non-

linearities that neocortical neurons could compute. The results of these experiments may have profound implications for theories of function of the neocortex.

5.3.2 Spike Initiation

The initiation of an all-or-none action potential is the point at which a neural signal is transformed from analog to pulse-coded information. The site at which this transformation occurs is critical to the nature of signal processing carried out by a neuron. A number of modeling studies have examined the possibility of dendritic spike initiation (e.g., Shepherd et al. 1985; Softky and Koch 1993; Softky 1994). This work has been based less on physiological data than on the appeal of the richer computational properties offered by nonlinear processing in dendrites. For example, using simulations, Shepherd et al. (1985) showed that the presence of Hodgkin-Huxley conductances in dendritic spines could give rise to nonlinear interactions between neighboring synaptic inputs, as well as saltatory dendritic conduction of action potentials. Similarly, Softky (1994) modeled a mechanism for submillisecond synaptic coincidence detection based on brief dendritic spikes carried by fast Na^+ and K^+ currents. The relevance of speculative proposals such as these depends critically on resolving the actual locus of spike initiation.

In the classical description of spike initiation derived from the motoneuron, initiation normally occurs in proximal segments of the axon (in the region of the axon hillock or initial segment); when orthodromic stimulation is increased, the site of initiation may move into the dendrites (Coombs, Curtis, and Eccles 1957b; Fatt 1957; Fuortes, Frank, and Becker 1957). In the hippocampus and neocortex, the possibly greater excitability of pyramidal cell dendrites could tend to favor dendritic spike initiation (Spencer and Kandel 1961).

Both orthodromic and antidromic dendritic spike propagation in the hippocampus were described originally using current source density measurements (Richardson, Turner, and Miller 1987; Turner et al. 1991; Turner, Meyers, and Barker 1993). Dual dendritic/somatic recordings confirmed that the axon is a preferential site for spike initiation in neocortical and hippocampal pyramidal cells (Stuart and Sakmann 1994; Spruston, Jonas, and Sakmann 1995; Colbert and Johnston 1996), but that dendritic spike initiation can occur in mature animals during strong synaptic stimulation (Turner et al. 1991; Regehr et al. 1993; Stuart and Sakmann 1996).

When spikes initiate first in the axon, the action potential backpropagates into the dendritic tree (Turner et al. 1991; Stuart and Sakmann 1994). This antidromically propagating action potential could signal the firing time of the neuron throughout the dendritic arbor, leading, for example, to Hebbian plasticity (Markram et al. 1997; Magee and Johnston 1997). The degree of invasion of the backpropagating

action potential is not fixed (Spruston, Jonas, and Sakmann 1995; Svoboda et al. 1997) but can be regulated through Na^+ channel inactivation by previous spikes (modeled by Migliore 1996), K^+ channel activation, excitatory (Magee and Johnston 1997; Hoffman et al. 1997) or inhibitory (Buzsaki et al. 1996; Tsubokawa and Ross 1996) synaptic potentials, and, potentially, neuromodulators such as acetylcholine, norepinephrine, and serotonin.

Two recent modeling studies of spike initiation have attempted to account for the above experimental results using known anatomical and physiological properties of pyramidal cells (Mainen et al. 1995; Rapp, Yarom, and Segev 1996). Both studies used reconstructed cortical neurons and just two voltage-dependent currents, I_{Na} and I_{Kd}, assuming that the contributions from the other currents would not be significant during on the short time scale of spike initiation. The conclusions of the two studies were similar (figure 5.3):

1. The passive electrical load biases the neuron toward spike propagation in the antidromic direction. This is analogous to the greater ease with which a voltage signal is passed outward from the soma than inward toward the soma, (see chapter 2, this volume) although geometrical considerations alone are insufficient to account for a strong bias for axonal initiation.

2. The presence of a larger source of Na^+ current—either a very high density (Mainen et al. 1995) or a moderate density with altered kinetics (Rapp, Yarom, and Segev 1996)—in the axon initial segment can account for preferential axonal initiation (but compare with Colbert and Johnston 1996, discussed earlier).

3. Although density measurements for the dendritic and somatic Na^+ channels are similar (Stuart and Sakmann 1994), the experimentally observed decrement of the backpropagating spike can be reproduced because this density is low. The axonal Na^+ source serves to increase the amplitude of the somatic action potential.

4. A developmental increase in Na^+ density (Huguenard, Hamill, and Prince 1988) can account for the increased tendency toward dendritic initiation in older animals (Stuart and Sakmann 1996).

A recent physiological study (Hoffman et al. 1997) has shown that dendritic K^+ channels may also have a major role in the locus of initiation and control of dendritic action potential. An enrichment of an I_A-like current in the dendritic arbor (Maletic-Savatic, Lenn, and Trimmer 1995) can limit the size of transient events such as EPSPs and spikes, thereby shunting dendritic spikes. By activating during the rising phase of the action potential, this current could also reduce the amplitude of a backpropropagating spike, allowing for a relatively higher dendritic Na^+ current

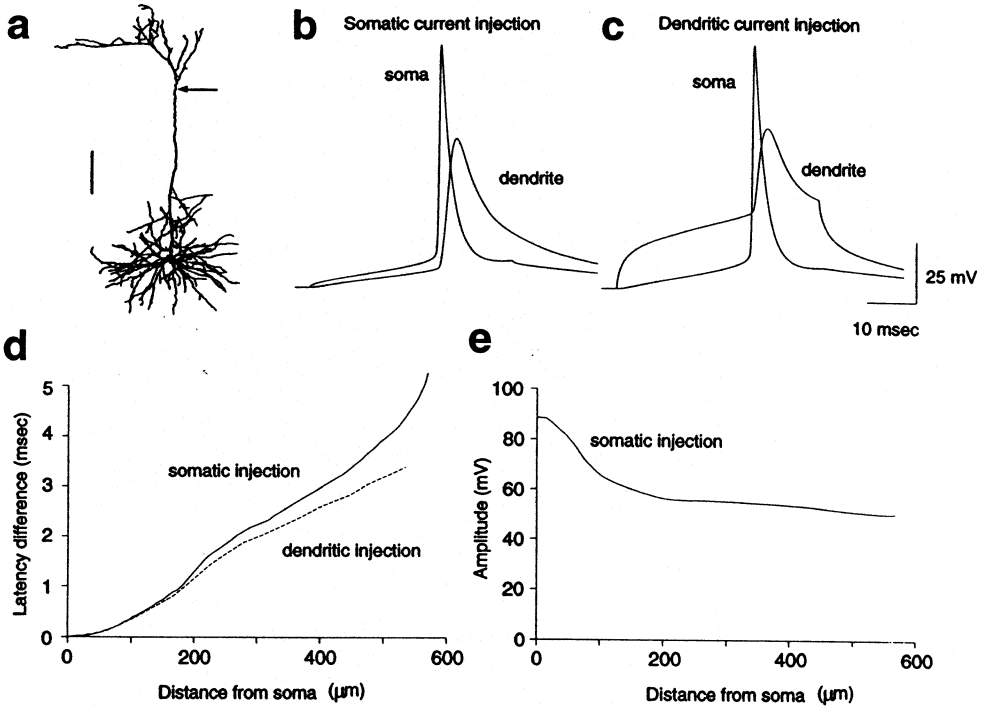

Figure 5.3
Site of action potential initiation in a model of a neocortical pyramidal neuron (compare to Stuart and Sakmann 1994, figure 1). (a) Digitally reconstructed layer-5 pyramidal neuron (courtesy of D. K. Smetters and S. Nelson, unpublished). Arrow indicates dendritic recording/stimulation site in panels b–c. Scale bar is 100 μm. (b) Simulation of action potentials evoked by a current step injected at the soma. Voltage traces from the soma and apical dendrite are shown. (c) Similar to panel b, but current injection is made at the dendritic site. (d) Latency difference between peak somatic and peak dendritic potential at different distances from the soma. Action potentials were elicited by somatic (solid line) or dendritic (dashed line) current injection. Latencies were measured using time-to-peak amplitude. (e) Action potential amplitude plotted as function of distance from the soma under the same conditions as in panel b following somatic injection. This figure is based on Mainen et al. 1995. NEURON code, including ".mod" files describing the active currents and ".hoc" code describing the morphologies and simulation setup, used to generate this figure is available; see "Internet Resources."

density, even while maintaining a decremental antidromic invasion (Hoffman et al. 1997).

In contrast to the many models that explore the consequences of Na^+ and Ca^{2+} currents in dendrites, models that explore the functional roles of dendritic K^+ currents have been few (e.g., Wilson 1995; Hoffman et al. 1997), in part because patch recordings and anatomical studies of K^+ currents are not as far advanced (Softky and Koch 1993; Bernander, Koch, and Douglas 1994; Wilson 1995; Andreasen and Lambert 1995). Both Rapp, Yarom, and Segev (1996) and Mainen et al. (1995) used a low density of dendritic K^+ channels to reproduce the relatively slow repolarization of the dendritic spike and the lack of AHP in the dendrites (Stuart and Sakmann 1994). However an I_A that inactivates rapidly enough may exert its influence primarily on the upstroke of a dendritic spike and become inactivated without contributing to a fast repolarization or AHP (Hoffman et al. 1997).

Given the importance of spike initiation for cortical signaling—all the information that flows into, out of, and between cortical areas is coded by spike trains—the axon hillock and initial segment deserve much more attention.

5.3.3 Intrinsic Firing Patterns

Different types of neurons produce different intrinsic rhythmic firing patterns when stimulated with a simple depolarizing current pulse in vitro in the absence of synaptic activity. For pyramidal neurons, these intrinsic patterns are typically either bursting (stereotyped clusters of two or more spikes firing at rates of up to 1,000 Hz) or adapting (firing at rapidly or gradually slowing rates; McCormick et al. 1985). The impression of these intrinsic properties can be seen in the characteristic firing modes of different types of neurons in vivo (e.g., complex spikes fired by hippocamal pyramidal cells, which relect their intrinsic bursting properties). Thus the temporal pattern of spikes emitted by a neuron in vivo reflects both the pattern of synaptic and modulatory input the neuron receives and the sculpting of this input by the dendritic, somatic, and axonal conductances that generate the spike train (Llinás 1988).

Modeling (and experimental) studies have begun to explore three important issues in the relationship between intrinsic firing patterns and neural signaling:

1. How are intrinsic firing patterns determined by the interplay of intrinsic conductances and neural geometry (see below)?

2. How do intrinsic currents interact with synaptic currents (e.g., Reyes and Fetz 1993; De Schutter and Bower 1994b, 1994c; Jaeger, De Shutter, and Bower 1997; Mainen and Sejnowski 1995; Tang, Bartels, and Sejnowski 1997)?

3. How do different temporal spike patterns interact with the filtering characteristics of synaptic transmission (e.g., Markram and Tsodyks 1996; Tsodyks and Markram 1997; Abbott et al. 1997; Lisman 1997)?

While all three issues are crucial to understanding the propagation of a neural signal, with respect to the modeling literature, the first is by far the best developed.

Models of bursting and repetitive firing in pyramidal neurons were pioneered by Traub and colleagues (Traub and Llinás 1979; Traub 1979, 1982; Traub et al. 1991, 1994). The original Traub model (Traub and Llinás 1979) laid out basic mechanisms by which slow dendritic Ca^{2+} and K^+ channels, partially coupled with somatic Na^+ channels, gave rise to rhythmic bursting in hippocampal pyramidal neurons. This model also documented the ability of dendritic Na^+ "hot spots" on fine dendrites to produce the fast prepotentials described in these neurons (Spencer and Kandel 1961). A revision of this model (Traub 1982) was constructed to account for data showing bursts generated locally in the dendrites (Wong, Prince, and Basraum 1979); this required the addition of dendritic inactivating K^+ conductances (I_A), a prediction that appears to have been borne out by the recent data (Hoffman et al. 1997).

The elaboration of the bursting model in Traub et al. (1994), which included an axon and more complex dendrites, combined synaptic and intrinsic voltage-dependent conductances. Versions of the Traub model have served as the starting point for other models aimed at exploring the influence of intrinsic properties of neurons on the interactions between neurons in area CA3 of the hippocampus. The model CA3 pyramidal neuron was also modified to serve as a CA1 pyramidal neuron by increasing I_{Kd} and decreasing dendritic I_{Ca} and I_C. After these alterations, tonic depolarization of the soma leads to adapting repetitive firing, whereas stimulation of the distal dendrites leads to bursting. A related model of bursting in neocortical neurons emphasized the importance of dendritic I_{Na} in propagating the somatic spike into the dendrites to trigger I_{Ca} (Rhodes and Gray 1994). Bursting in this model depended critically on the amount of I_{AHP} activation, and hence on the level of intracellular Ca^{2+}.

In these models of bursting, the Ca^{2+} currents in the dendrites produce the prolonged depolarization that initiates the fast Na^+ spikes, but there is increasing evidence that Na^+ currents themselves can produce bursts in some neurons (Turner et al. 1994; Franceschetti et al. 1995; Azouz, Jensen, and Yaari 1996). Because Na^+ currents are quite brief, the longer time scale of the burst must arise somehow from the geometry of the neuron and the interaction between different conductances in different compartments. Using reconstructed cortical neurons with different dendritic structures but a fixed distribution of ion channels, Mainen and Sejnowski (1996)

have shown that the entire range of intrinsic firing patterns, including nonadapting, adapting, and bursting types, can be reproduced in a set of neurons that differ only in their geometry (figure 5.4). In their study, reconstructed layer-5 pyramidal cells with large dendritic arbors produced repetitive bursting to current injection, while more compact layer 2/3 pyramidal cells produced regular spiking behavior. These results demonstrated that the electrotonic structure of a neuron shapes the dynamic interactions between nonuniformly distributed ion channels, and may thereby shape the pattern of repetitive firing. The wide anatomical variety of neocortical dendrites (Peters and Jones 1984), supported the idea of a continuous spectrum of neocortical firing patterns (McCormick et al. 1985; Connors and Gutnick 1990), rather than discrete categories.

Mainen and Sejnowski (1996) suggested a causal relationship for the observed correlations between dendritic structure and firing properties (Connors and Gutnick 1990; Chagnac-Amitai, Luhmann, and Prince 1990; Mason and Larkman 1990; Franceschetti et al. 1995; Yang, Seamans, and Gorelova 1996) and emphasized the importance of active dendritic conductances in neuronal function. Quadroni and Knöpfel (1994) have also demonstrated in simulations that the number of dendrites may affect the firing patterns of medial vestibular neurons. Heterogeneity of dendritic structure can thus parsimoniously explain some aspects of the heterogeneous firing properties of neurons in terms of their anatomical diversity, but heterogeneity in the distribution of channel may also be important. Indeed, a modeling study by Migliore, Alicata, and Ayala (1995) demonstrated that the effects of small differences in morphology can be overridden by tuning the relative densities of intrinsic currents such as sI_{AHP}.

Most of these models are based on data from cortical slices that lack the spontaneous background firing activity and tonic neuromodulation that occurs in vivo. Models that take these conditions into account (Bernander et al. 1991; Rapp, Yarom, and Segev 1992; Tang, Bartels, and Sejnowski 1997) may reveal other properties of neurons that are important for their participation in perceptual and cognitive states.

5.4 Analysis

This chapter has focused on highly detailed models of pyramidal cells derived from anatomical and physiological data. The resulting models of active dendritic processes are complex, yet, however exhaustively their behavior may be scrutinized, new tools for analysis may be needed to achieve a deeper understanding of the phenomena they display. The development of these methods is still nascent, but several useful avenues are worth mentioning.

5.4.1 Reduced Models

If the complex behavior of a realistic model can be captured in a much simplified version of the model, understanding of the model can be enormously improved. Collapsing the number of compartments in a model is a good starting point for simplification. For passive electrical structures, several straightforward methods are discussed in chapter 3, this volume. With active models, reducing both the number of active conductances and the number of compartments may be useful (e.g., Lytton and Sejnowski 1991; chapter 10, this volume).

A single-compartment model will be sufficient when the electrotonic structure of the neuron is not relevant to its behavior, but otherwise, a minimal model consists of two compartments. Pinsky and Rinzel (1994) developed a simplification of the model of Traub et al. (1991) with just two compartments, identified as a soma and a dendrite. The electrical geometry was reduced to two parameters: the ratio of soma to dendrite area, ρ; and the coupling resistance between then, κ. Despite this simplicity, the model captured essential aspects of the generation of bursting in the Traub model not found in a single-compartment model (Pinsky and Rinzel 1994). The reduced number of parameters allows the model to be used efficiently in network simulations and aids in understanding the role played by electrical structure in the behavior of the model. (See more in chapter 10, this volume.)

Mainen and Sejnowski (1996) also used a two-compartment model similar to that of Pinsky and Rinzel (1994) to elucidate the effects of electrical geometry on the firing patterns of neocortical neurons. The full range of regular spiking responses, adaptation, afterdepolarizations, and repetitive bursting observed in recordings and in models of reconstructed pyramidal cells and inhibitory neurons could be reproduced in the two-compartment model. This reduced model shed light on the mechanisms responsible for the effects of geometry on the spike firing pattern observed in more detailed models of reconstructed neurons.

5.4.2 Current-Voltage Curves

One of the more informative analyses for understanding how a model neuron will respond to inputs is the current-voltage relationship (I-V curve). Because data from experimental recordings are often presented in this way, the I-V curve of the model can be compared directly with measurements. The steady-state, or static I-V curve, $I_{\infty}^{static}(V_m)$, is obtained by voltage clamping the soma to V_m and determining the asymptotic current. The slope of this curve defines the steady-state input conductance of the neuron as a function of membrane potential. The momentary, or instantaneous, I-V curve, $I_O(V_m)$, is obtained by changing the membrane potential

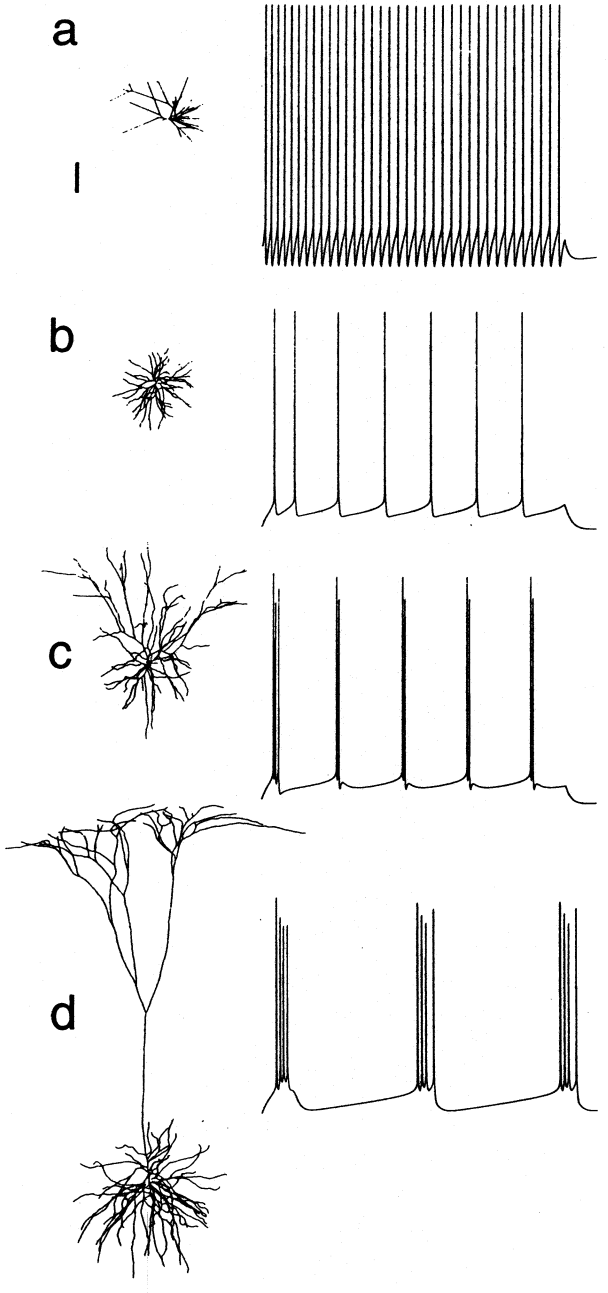
a
I
b
c
d

rapidly from the resting level to a new value, V_m, more rapidly than all the conductances (except for I_{Na}, which has an activation time of less than 100 μsec).

Koch, Bernander, and Douglas (1995) have analyzed the threshold of a model cortical pyramidal cell using the I-V relationships (figure 5.5). Near the spiking threshold, there is a local maximum in the $I_{\infty}^{static}(V_m)$, which corresponds to the current threshold for sustained inputs. The voltage threshold, which applies to rapid synaptic currents or current injection, occurs at a zero-crossing of $I_O(V_m)$, which is more depolarized than $I_{\infty}^{static}(V_m)$. Koch, Bernander, and Douglas (1995) define a third, dynamic I-V relationship, while the cell is spiking. The relationship between current inputs in the dendrites and spiking in the soma can also be studied using similar techniques (Jaeger, De Schutter, and Bower 1997).

5.4.3 Phase Plane Analysis

Because the previous histories of the ionic currents are also important in determining the response of a neuron to an input, the I-V curves defined above only give a rough idea of how a cell will respond to a more complex time-varying input. Hysteresis occurs already at the start of a simulation because the states of the activation and inactivation variables of all the ionic currents affect the subsequent dynamics. Phase plane analysis can be used to visualize and analyze the complex dynamics exhibited by neurons during simulations.

The "phase" in phase plane analysis refers to variables such as the membrane potential and current that dynamically change during a simulation but it also includes other variables such as the activation and inactivation variables for the ionic currents and ion concentrations. In the phase plane of current against membrane potential, the neuron follows a trajectory on a two-dimensional graph (see chapter 7, this volume). The current through specific channels or the internal Ca^{2+} concentration can also serve as axes in a phase plane. For example, Lytton and Sejnowski

Figure 5.4
Distinct firing patterns in model neurons with identical channel distributions but different dendritic morphology. Digital reconstructions of dendritic arbors of neurons from rat somatosensory cortex (panel a) and cat visual cortex (panels b–d). (a) Layer-3 aspiny stellate. (b) Layer-4 spiny stellate. (c) Layer-3 pyramid. (d) Layer-5 pyramid. Somatic current injection evoked characteristic firing patterns. Panel a shows only the branch lengths and connectivity, while panels b–d show a two-dimensional projection of the three-dimensional reconstruction. Scale bars: 250 μm (anatomy), 100 msec, 25 mV. Dendritic reconstructions were provided by J. Anderson, K. Martin, R. Douglas, L. Cauller, and B. Connors. Active conductances included four active currents: I_{Na} from Mainen et al. 1995; I_{Kd} from Mainen et al. 1995; I_M from Gutfreund, Yarom, and Segev 1995; I_{Ca} from Reuveni et al. 1993; and sI_{AHP} from Reuveni et al. 1993. This figure is based on Mainen and Sejnowski 1996. NEURON code, including ".mod" files describing the active currents and ".hoc" code describing the morphologies and simulation setup, used to generate this figure is available; see "Internet Resources."

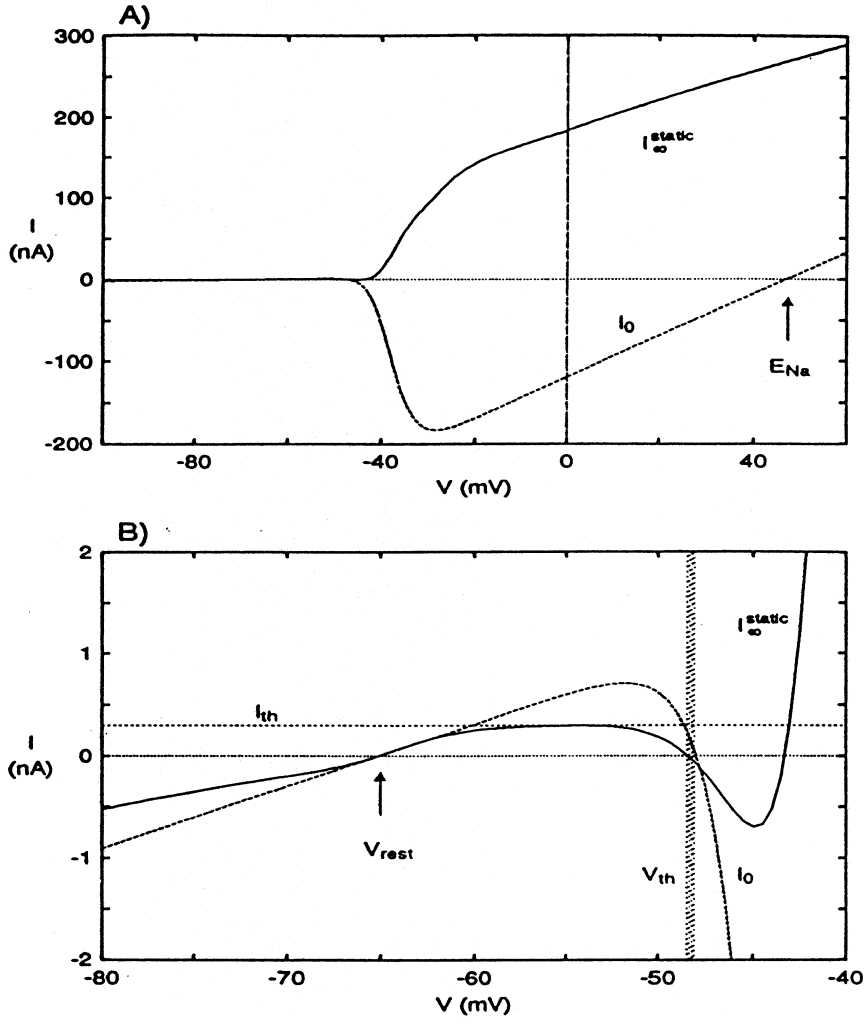

Figure 5.5
Current-voltage relationship for a model cell (Koch, Bernaabe and Douglas, 1995). The somatic membrane potential V_m was voltage-clamped and the clamp current '$I_\infty^{static}(V_m)$', recorded once steady state was reached. The instantaneous current-voltage curve '$I_0(V_m)$', assumes that the membrane potential is instantaneously displaced from V_{rest} to its new value at V_m. All somatic membrane conductances retain the values they had at V_{rest} with the sole exception of the fast sodium activation process—due to its very fast time constant (50 μsec) we assume that it reaches its steady-state value at V_m. (A) Full range. Note the very large amplitudes of I_0 (due to I_{Na} activation) and of $I_\infty^{static}(V_m)$ (due to I_{Dr} activation). The instantaneous current I_0 crosses over close to the reversal potential for I_{Na}. (B) Detail of panel A in the vicinity of the resting potential and spike threshold. Both curves reserves at V_{rest}. The slope of $I_\infty^{static}(V_m)$ corresponds to the inverse of the input resistance at rest. The right zero-crossing of I_0 occurs at $V_m = -48$ mV and that of $I_\infty^{static}(V_m)$ at -48.5 mV. The amplitude of $I_\infty^{static}(V_m)$ at the local peak around -54 mV represents the current threshold, I_{th}, for spike initiation, while the location of the middle zero-crossing of I_0 corresponds to the voltage threshold V_{th} for spike initiation (indicated by the thin gray area).

(1991) used phase plane analysis with these variables to explore the entrainment of cortical pyramidal neurons by inhibitory postsynaptic potentials. In some cases it is possible to gain a qualitative feel for the dynamics by plotting the null clines on the phase plane, which correspond to lines along which the derivatives of variables are zero (Murray 1989).

Phase plane analysis can reveal more about the mechanisms underlying dynamics through the application of bifurcation theory. As one parameter, such as input current or a conductance, is changed slowly, the phase plane trajectory for a repetitively firing neuron may qualitatively shift, for example, from a regular spiking mode to a bursting mode (see chapter 7, this volume; Butera, Clark, and Byrne 1996). This sudden shift indicates that a bifurcation has occurred in the dynamics; that is, a discontinuous change in the behavior of the system. In the theory of dynamical systems, the types of bifurcations that can occur have been classified and analyzed. Although this approach is normally used on simplified models of neurons that can be characterized by a few differential equations, new automated software systems such as XPP (Bard Ermentrout; see chapter 7, this volume; ftp://ftp.math.pitt.edu/pub/bardware/tut/start.htm) and "DsTool" (John Guckenheimer; ftp://macomb.tn.cornell.edu/pub/dstool) make it feasible to analyze the bifurcations in more realistic models systems represented by dozens of differential equations.

Internet Resources

An increasing number of valuable resources are available on the Internet. At our web site, http://www.cnl.salk.edu/CNL/simulations/methods.html, we have compiled a directory that includes code used to generate several of the models illustrated here (figures 5.3 and 5.4), as well as links to simulation software (e.g., NEURON and GENESIS) and models. This directory will be periodically updated.

Acknowledgments

The preparation of this chapter was supported by Howard Hughes Medical Institute, National Institutes of Health, and the Office of Naval Research. We are grateful to Venkatesh Murthy and Brian Christie for comments on this chapter.